Electron-Transfer Dynamics of Photosynthetic Reaction Centers in Thermoresponsive Soft Materials

Philip D. Laible,[†] Richard F. Kelley,[‡] Michael R. Wasielewski,[‡] and Millicent A. Firestone*[,§]

Biosciences and Materials Sciences Divisions, Argonne National Laboratory, Argonne, Illinois 60439, and Department of Chemistry and Center for Nanofabrication and Molecular Self-Assembly, Northwestern University, Evanston, Illinois 60208-3113

Received: July 14, 2005; In Final Form: September 7, 2005

Poly(ethylene glycol)-grafted, lipid-based, thermoresponsive, soft nanostructures are shown to serve as scaffolding into which reconstituted integral membrane proteins, such as the bacterial photosynthetic reaction centers (RCs) can be stabilized, and their packing arrangement, and hence photophysical properties, can be controlled. The self-assembled nanostructures exist in two distinct states: a liquid-crystalline gel phase at temperatures above 21°C and a non-birefringent, reduced viscosity state at lower temperatures. Characterization of the effect of protein introduction on the mesoscopic structure of the materials by ^{31}P NMR and small-angle X-ray scattering shows that the expanded lamellar structure of the protein-free material is retained. At reduced temperatures, however, the aggregate structure is found to convert from a two-dimensional normal hexagonal structure to a three-dimensional cubic phase upon introduction of the RCs. Structural and functional characteristics of the RCs were determined by ground-state and femtosecond transient absorption spectroscopy. Time-resolved results indicate that the kinetics of primary electron transfer for the RCs in the low-viscosity cold phase of the self-assembled nanostructures are identical to those observed in a detergent-solubilized state in buffered aqueous solutions (∼4 ps) over a wide range of protein concentrations and experimental conditions. This is also true for RCs held within the lamellar gel phase at low protein concentrations and at short sample storage times. In contrast are kinetics from samples that are prepared with high RC concentrations and stored for several hours, which display additional kinetic components with extended electron-transfer times (∼10−12 ps). This observation is tentatively attributed to energy transfer between RCs that have laterally (in-plane) organized within the lipid bilayers of the lamellar gel phase prior to charge separation. These results not only demonstrate the use of soft nanostructures as a matrix in which to stabilize and organize membrane proteins but also suggest the possibility of using them to control the interactions between proteins and thus to tune their collective optical/electronic properties.

Introduction

The development of synthetic, biomembrane-mimetic materials that can house membrane proteins with retention of their native structure and activity would both advance the fundamental understanding of membrane protein structure and function and offer the possibility of harnessing proteins for use in nanoscale devices. Membrane proteins facilitate many key cellular processes, including signal recognition, ion transport, and energy transduction. In effect, they possess all of the basic properties necessary for the construction of nanoscale devices appropriate for any of a variety of tasks, including optical/electronic signal amplification, switching, gating, data storage, sensing, and energy storage and conversion.[1−6] The use of membrane proteins as the basis for functional nanoscale devices, however, has received considerably less attention than have water-soluble proteins, a result of the lack of materials allowing for their structural and functional stabilization outside of their native environment. To date, surface-supported approaches (Langmuir−Blodgett, self-assembled monolayers, solid-supported lipid bilayers)[3−5] have been the primary means of preparing ordered arrays (ensembles) of membrane proteins. These solid-supported biomembrane-mimetic strategies suffer from several limitations, namely, blocked access to one side of the membrane and insufficient space between the bilayer and the surface, often resulting in reduced or altered functionality of the reconstituted protein. Recent efforts have been directed at developing bulk materials, including sol−gel or mesoporous hosts,[6] incorporating membrane proteins. To date, these materials have not been optimized and do not yield ordered protein arrays. These studies clearly demonstrate the need for new materials that can house, order, and control encapsulated membrane protein arrays.

Photoactive membrane proteins derived either from bacterial photosynthetic systems such as reaction centers (RCs) or bacteriorhodopsin (bR), or from high-order green plants such as photosystem I or II have received the most attention, since these proteins represent promising candidates for use in solar cells, photonic materials, and optoelectronics.[3] The successful use of photoactive membrane proteins requires, first and foremost, their stabilization in an optically transparent, nondenaturing environment that allows for control of their orientation and ordering within the matrix. Ultimately, for many areas of application, they will also need to be interfaced to current device architectures. In this work, we consider the first of these material

* Author to whom correspondence should be addressed. Phone: (630) 252-8298. Fax: (630) 252-9151. E-mail: firestone@anl.gov.
[†] Biosciences Division, Argonne National Laboratory.
[‡] Northwestern University.
[§] Materials Science Division.

10.1021/jp053884n CCC: $30.25
Published on Web 11/15/2005

design issues by evaluating the stability, organization, and photophysics of bacterial photosynthetic reaction centers encapsulated in thermoresponsive, soft nanostructures.

These poly(ethylene glycol) (PEG)-grafted, lipid-based nanostructures (complex fluids[7]) are comprised of a mixture of three molecular components—a saturated phospholipid (e.g., dimyristoylphosphatidycholine (DMPC)), a polymer (here introduced as a lipopolymer, PEGylated dimyristoylphosphatidylethanolamine (DMPE-EO_{45})), and a cosurfactant (e.g., *N*,*N*-dimethyldodecylamine-*N*-oxide (LDAO))—that spontaneously self-assemble into noncovalent aggregates when dispersed in water.[8] These assemblies are both uniform and optically transparent in the visible to near-infrared (NIR) region of the spectrum. Furthermore, they undergo a thermoreversible phase transition, converting between an optically birefringent, gel, lamellar phase ($L_\alpha g$) above the phase transition ($T_m = 21°C$) and a non-birefringent, low-viscosity, two-dimensional (2D) hexagonally ordered array of prolate micelles (H_1) at lower temperatures. Both phases feature lattice dimensions on the order of hundreds of nanometers that are tunable over a wide range by simply changing either the water content or the number of repeat units on the appended PEG chains. Moreover, the lamellar gel phase architecture (i.e., lipid bilayer) mimics that of a native cell membrane. The inverted phase transition exhibited by this material (i.e., liquid phase at a lower temperature than the gel phase) is unique among biomembrane-mimetic systems and, as our prior work has shown,[8−10] allows for the introduction and admixing of delicate biomolecules in the low-viscosity (cold) state.[11] Subsequent warming of the sample to room temperature promotes the partitioning and self-organization of the biomolecules into either the aqueous (in the case of soluble proteins) or the alkyl chain bilayer domains (for membrane proteins).[11] Our subsequent work has also demonstrated that exploitation of the inverted phase transition in the presence of an applied magnetic field provides a facile means of aligning the lamellar microdomains, thereby eliminating unfavorable orientations and defects in these materials and extending the order into macroscopic dimensions.[9]

In the present work, we evaluate the applicability of these thermoresponsive soft nanostructures in organizing a model light-transducing membrane protein, the RC. Specifically, the stability and photophysics of the RC in the two distinct phases afforded by the complex fluids are evaluated and compared to the RC behavior in a well-characterized, detergent-solublized state (i.e, in buffered aqueous solution). Our results demonstrate that the RC is stable in both phases of the complex fluid and suggest that protein functioning may be modulated by the environment afforded by the lamellar gel phase of the complex fluid.

Experimental Section

Complex Fluids. Complex fluids were prepared as previously described.[8] The quaternary compositions consisted of 0.823 ± 0.001 weight fraction water or 10 mM Tris, 50 mM NaCl buffer pH 7.8 (Φ_w), 0.023 ± 0.0015 weight fraction surfactant (Φ_s, lauryldimethylamine-*N*-oxide (LDAO) purchased from Calbiochem-Novabiochem Corp., (LaJolla, CA)), 0.154 ± 0.0210 weight fraction lipid (Φ_L, lyophilized 1,2-dimyristoyl-*sn*-glycerol-3-phosphocholine (DMPC) and 1,2-dimyristoyl-*sn*-glycerol-3-phosphoethanolamine-*N*-poly(ethylene glycol) (DMPE-EO_{45}) purchased from Avanti Polar Lipids (Alabaster, AL) and used as received). All samples were prepared such that the polymer-to-phospholipid ratio was held at 8 mol %. Hydration of the solid components with deionized water was accomplished by many repeated cycles of heating (50°C), vortex mixing, and cooling on an ice bath until sample uniformity was achieved.

Photosynthetic Reaction Centers. Native RCs (referred to as "wild-type" (WT)) with a polyhistidine tag appended to the C-terminus of the M subunit were prepared using affinity chromatography as previously described.[12] The site-specific mutant of the *Rhodobacter sphaeroides* M gene (change from the native Trp codon TGG at position 252 to the Valine codon GTG; M252Trp → Val) was constructed specifically for this study by oligonucleotide-directed mutagenesis according to instructions from a kit (QuikChange, Stratagene). The two-base-pair replacement introduced a nonunique *Hae*II site that was used for screening purposes. Template plasmids containing the histidine-tagged, *R. sphaeroides* RC-M gene have been previously described.[12] Subsequently, the mutant M gene was substituted for an *Mlu*I-tagged version of the native M gene in a previously constructed expression system. The presence of the desired substitution was confirmed by DNA sequencing (MWG-Biotech). The *Rhodobacter* strain that produced the mutant RCs was grown under chemoheterotrophic conditions (semiaerobic, dark, 34°C) in rich medium, YCC,[13] containing 1 mg/mL tetracycline to ensure retention of the expression plasmid. Detergent-isolated RCs were prepared by affinity chromatography and buffer exchange methods in the presence of LDAO.[12,14] The purified samples were concentrated to an A_{800} of 60−80 (1 cm path, 20−28 mg/mL) using a centrifugal concentrator (2000*g*, 50 kDa cutoff membrane (Millipore)) and were flash frozen in liquid nitrogen and subsequently stored at −80 °C for later use in spectroscopic or scattering experiments.

Proteo-Complex Fluids. Proteo-complex fluids containing the photosynthetic reaction centers were prepared by the introduction of the purified protein into a preformulation of the complex fluid (that is, one that compositionally corrects for the additional water and detergent introduced by the protein detergent complex).[11] Quantitative protein incorporation was facilitated by the low-viscosity, cold phase with dissolution promoted by gentle agitation. Thermal cycling of the proteo-complex fluid between 3 and 25 °C was carried out until a transparent, deep purple sample was prepared.

Physical Methods. Steady-state absorption spectra were obtained using a Shimadzu 1601 UV/vis/NIR spectrophotometer. Thermal properties were measured by differential scanning calorimetry (DSC) at heating rates of 2 °C/min on a TA Instruments Q100 interfaced to a refrigerated cooling system. Instrument calibration was performed using an indium standard. Weighed amounts (5−10 mg) of the complex fluids were sealed in aluminum pans and equilibrated at 3 °C for 10 min. Phase transitions were recorded over a range from 3 to 70 °C. Successive heating scans were found to yield identical results. The transition temperature (T_m) was taken as the temperature at the peak of the endothermic transition. Static, broad-band, proton-decoupled ^{31}P NMR spectra were recorded at 121.65 MHz on a GE Omega 300 spectrometer using a 70° response factor pulse width (8 ms) repeated every 2 s. Temperature control was achieved by dry-ice-cooled, N_2 gas flow. The free induction decays consisted of 160 scans and were multiplied by 50 Hz line broadening before Fourier transformation. Small-angle X-ray scattering (SAXS) measurements were made using the instrument at undulator beamline 12ID-C (11 keV) of the Advanced Photon Source at Argonne National Laboratory. The sample-to-detector distance was such as to provide a detecting range for momentum transfer of $0.0025 < q < 0.6$ Å^{-1}. The scattering vector, q, was calibrated using a silver behenate standard at $q = 1.076$ Å^{-1}. The 2D scattering images were first

corrected for spatial distortion and sensitivity of the detector and then radially averaged to produce plots of scattered intensity, $I(q)$, versus scattering vector, q, where is $q = 4\pi/\lambda(\sin\theta)$. The value of q is proportional to the inverse of the length scale, $Å^{-1}$. For these measurements, samples were sealed in 1.5 mm quartz capillaries. Temperature control of samples was achieved using a custom-built Peltier cooler.

Time-Resolved Spectroscopy. Femtosecond transient absorption measurements were made using a regeneratively amplified titanium sapphire laser system operating at a 2 kHz repetition rate outfitted with a charge coupled device (CCD) array detector (Ocean Optics PC2000) that allowed for simultaneous collection of spectral and kinetic data. The fundamental output of the laser provides 838 nm, 120 fs pulses for excitation. Focusing a few microjoules of the 838 nm light into a 1 mm sapphire disk generated a white light continuum probe pulse. All-reflective optics were used to focus the 838 nm pulses into the sapphire and recollimate the white light output, thus limiting the chirp on the probe pulses to <200 fs from 450 to 800 nm. The polarization of the probe beam was set at horizontal (0°) with respect to the lab frame of reference, while the pump polarization was set at the magic angle (54.7°) relative to the probe. The total instrument response function for the pump−probe experiments was 150 fs. Dual pathlength cuvettes were used to optimize thermal contact to the thermostated cell holder (Quantum Northwest Flash 100). The 0.1 mm pathlength orientation of the cuvettes was used for time resolved optical measurements. The samples were allowed to equilibrate for 15 min after reaching a particular temperature with variations less than 0.02 °C.[15] The thermostated cell holder was translated at a rate of ~40 μm/s to minimize photodegradation while collecting the entire kinetic data set in the course of one pass across the 1 cm width of the cuvette, in the plane perpendicular to the pump−probe beams during data acquisition, using a Zaber Technologies T-LA28 stepper motor. Five seconds of averaging were needed to obtain the transient spectrum at a given delay time. The samples were irradiated with 0.5 μJ per pulse focused to a 200 μm spot. The sample optical density at the excitation wavelength was ~0.3. Transient absorption kinetic profiles at a variety of wavelengths were fit to a sum of exponentials with a Gaussian instrument response function using Levenberg−Marquardt least-squares fitting.

Results and Discussion

In photosynthetic bacteria, the RC is responsible for the first step in conversion of light energy into a transmembrane, charge-separated state. The structure of the RC has been determined to near atomic resolution[16−22] and comprises a large (10^5 kDa), multi-subunit, transmembrane protein assembly. The RC complex is composed of transmembrane protein chains L and M and a mostly cytoplasmic polypeptide, H. The intramembrane cofactors that participate in sequential electron transfer consist of the dimer of bacteriochlorophyll (P), which serves as the primary electron donor, two bacteriochlorophyll monomers (B_A and B_B), two bacteriopheophytins (H_A and H_B), a non-heme iron atom, and two quinones (Q_A and Q_B), which serve as the final electron acceptors. An axis of approximate 2-fold symmetry relates the L and M chains as well as the set of cofactors that is bound to each chain (Figure 1, panel a). In the initial light-induced reactions, electron transfer in wild-type RCs proceeds from P to H_A within 3−4 ps and, subsequently, from H_A to Q_A within 200 ps.[23,24]

The room-temperature, ground-state absorption spectrum of an RC in the NIR region shows three major absorbance bands,

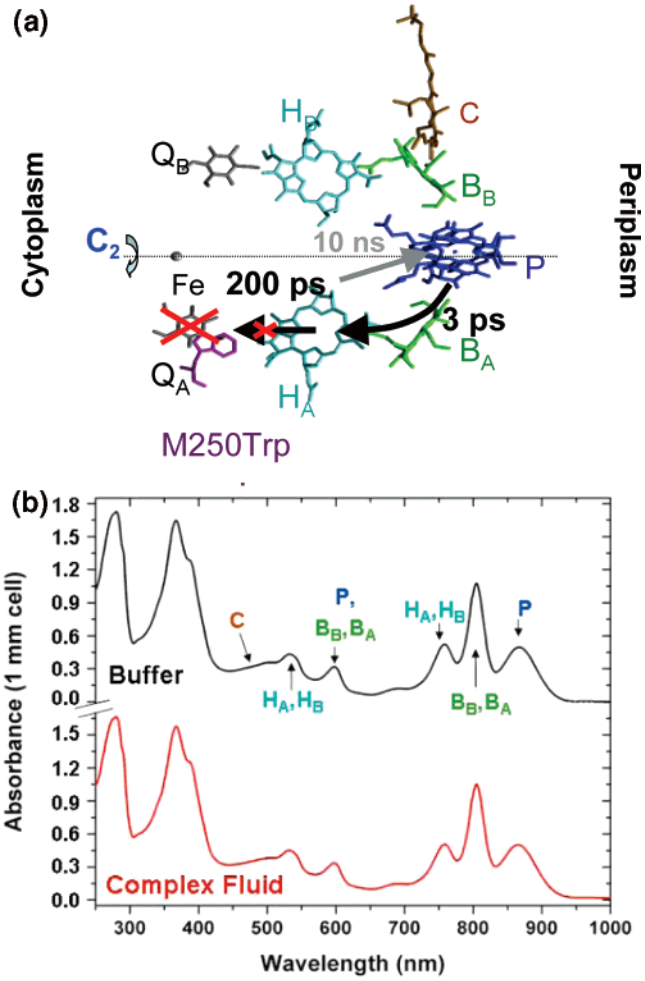

Figure 1. (a) Structural position of the substituted amino acid (M252Trp) in relation to the cofactors in the bacterial RC[19] with relevant pathways and time constants for multistep forward electron transfer (solid back arrows) and charge recombination (dashed gray arrow). (b) Steady-state absorption spectra of purified mutant reaction centers either suspended in detergent micelles (top, black) or as incorporated into the gel phase of a complex fluid (bottom, red).

the positions and intensities of which are sensitive to the integrity of the cofactors and local protein environment.[25] The introduction of wild-type or mutant RCs (in a detergent-solubilized state) into the preformed complex fluid in the cold phase produced an optically transparent, deep purple gel when warmed to room temperature. The structural integrity of the reaction centers within both phases of the complex fluid was determined by monitoring the relative position and intensity of the NIR absorption bands. Comparison of the NIR absorption spectra of detergent-solubilized RCs with the spectra of RCs reconstituted into both the lamellar gel phase (Figure 1, panel b) and the cold, reduced viscosity state of the complex fluid shows good correspondence between them, demonstrating that the reaction centers remain structurally intact upon introduction into the complex fluid.

Protein−Complex Fluid Interactions. The influence of WT-RC reconstitution on the properties and structure of the complex fluid was also examined. Specifically, thermal analysis was used to evaluate the nature of the RC-complex fluid interaction. The thermotropic phase behavior of lipid-membrane systems is known to be strongly influenced by the presence of guest molecules such as proteins. In particular, the thermally induced gel−liquid (L_β−L_α) phase transition is determined by the nature of the interactions between the membrane constituents and by

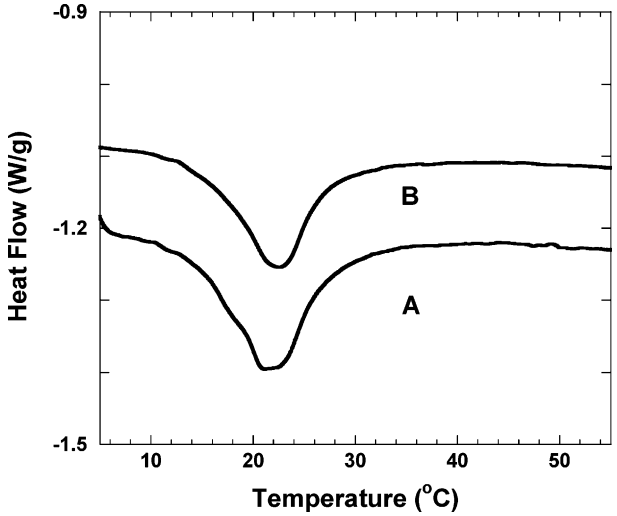

Figure 2. Calorimetric heating curves: (A) undoped; (B) RC (14.5 μM)-doped PEGylated lipid-based complex fluid compositions, scan rate 2 °C/min. Identical thermograms were obtained independent of the initial equilibration temperature.

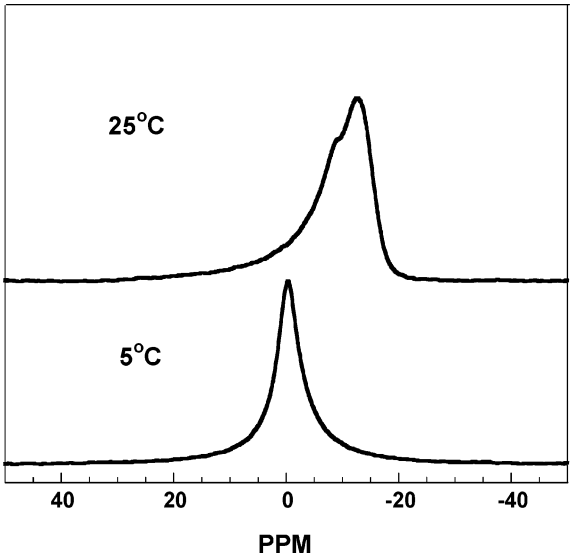

Figure 3. Phosphorus NMR spectra obtained at 122 MHz (7.05 T). PEGylated lipid-based complex fluid with RCs (16.9 μM), recorded as a function of temperature: (A) 25 °C; (B) 5 °C.

the general topology of the guest.[26] The DSC heating profile (Figure 2A) obtained for the undoped quaternary phase exhibits a complex phase transition in the temperature range of 14−30°C. This transition features a broad (full width at half-maxium (fwhm) is 7.2 °C), unsymmetrical profile comprising two components: a peak centered at $T_m = 21.1$ °C and a shoulder at ca. 16 °C. The thermogram recorded on a sample that has been reconstituted with RCs (14.5 μM) shows some minor differences (Figure 2B). In particular, a slight shift in the peak position is observed ($T_m = 22.4$ °C), and the transition is slightly narrowed relative to the undoped phase (fwhm is 6.7 °C). The observed changes in the thermal properties (i.e., an increase in T_m and a decrease in the width of the transition) suggest that the intercalated guest (protein) fits well into the membrane and acts synergistically to increase the local order and rigidity of the membrane.[27] Thus, the RCs are apparently well integrated into the lipid bilayer of the complex fluid. Moreover, the gross features of the complex fluid phase transition are preserved upon introduction of the protein.

To more fully determine the influence of protein introduction, it was necessary to characterize the structural states of the proteo-complex fluid both above and below the phase transition. The ^{31}P NMR line shape of aqueous dispersions of phospholipids has previously been demonstrated to serve as an effective diagnostic tool for distinguishing between lamellar and the various nonlamellar (e.g., hexagonal vs cubic) mesophase structures.[8,28,29] The differences in line shape, which provide a simple means to determine aggregate morphology, arise as a result of the different degrees of motional freedom of the phospatidylcholine and phosphatidylethanolamine headgroups possible in the various structural phases. Therefore, ^{31}P NMR was used to evaluate the molecular environment of the lipid components in the complex fluid and to infer the mesoscopic structure of the proteo-complex fluid at temperatures above and below the phase transition.

At 25 °C (i.e., the gel phase), the ^{31}P NMR spectrum of a complex fluid containing 16.9 μM RCs (Figure 3) possesses a characteristic broad (fwhm of 9.59 ppm) asymmetric ^{31}P line shape with a high-field peak (at $\delta = 12.56$ ppm) and a low-field shoulder (at $\delta = 8.72$ ppm). The observed spectrum agrees well with that of the undoped material and is characteristic of a lamellar structure.[8] At sample temperatures well below the phase transition (e.g., at 5 °C), that is, in the low-viscosity state, the observed ^{31}P resonance for the RC-doped complex fluid shifts downfield and is nearly symmetric about $\delta = -0.27$ ppm (Figure 3). In addition, the spectral envelope becomes notably narrower (fwhm is 5.13 ppm). Such isotropic (symmetric), narrow ^{31}P NMR signals have been previously observed for lipid assemblies and have been attributed to the formation of a cubic/micellar phase. In contrast, the ^{31}P resonance for the undoped, protein-free composition was found to shift downfield, and the spectral envelope undergoes a reversal in peak asymmetry, consistent with a 2D hexagonal aggregate structure.[8] Thus, the ^{31}P NMR indicates that at room temperature the protein-doped gel phase adopts a liquid-crystalline lamellar structure, while at reduced temperatures, the liquid phase is nonlamellar, possibly adopting a cubic structure.

Because the structure of the system cannot be determined unambiguously by ^{31}P NMR alone, the material was further investigated by small-angle X-ray scattering. SAXS studies comparing the mesophase architectures of the undoped and RC-doped materials above the phase transition (i.e., in the gel phase) support the NMR studies, demonstrating the retention of a lamellar structure. The SAXS profile collected on a RC-doped (23.8 μM) material (Figure 4A) at 25 °C features four diffraction peaks at integral-order spacing ($q = 0.0454, 0.0906, 0.137, 0.183$ Å^{-1}), consistent with a highly ordered lamellar structure featuring a d spacing of 138 Å. Several minor differences are observed between the scattering patterns of the undoped and doped materials. First, a slight increase in the breadth of the first-order peak is observed, suggesting that the presence of the protein leads to a minor reduction in spatial coherence (i.e., increased lattice disorder and orientational order) and hence more poorly aligned microdomains of lamellae.[30] Second, a minor reduction ($\Delta d \approx 7$ Å) in the interlamellar lattice spacing is observed for the RC-reconstituted materials, which may arise from an RC-induced reduction in the steric repulsion provided by the tethered PEG chains between opposing bilayers.[31] SAXS measurements made on the same samples below the phase transition, at 5 °C, also are in agreement with the ^{31}P NMR findings, indicating that the materials no longer adopt well-ordered lamellar structures (Figure 4B). Both SAXS patterns display two broad envelopes comprising multiple peaks. The SAXS data collected on the RC-doped material, while similar to data for the undoped material, do exhibit two low-angle peaks

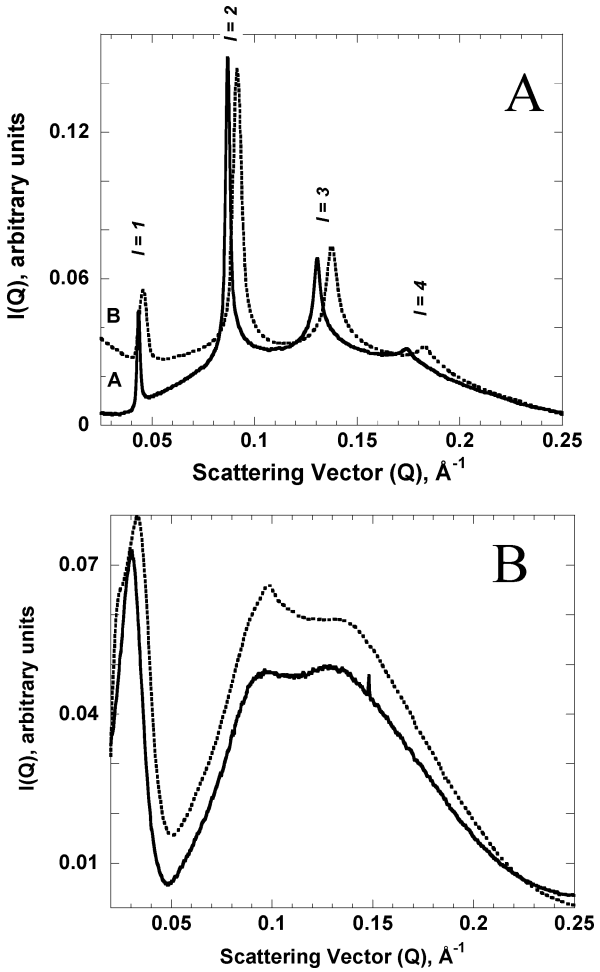

Figure 4. Small-angle X-ray scattering profile collected on undoped (solid line) and RC (23.8 μM)-doped gel (dashed line) phase at (A) 25 °C and (B) 3 °C.

(in the first envelope of diffraction) positioned approximately at 1:1; 1:$\sqrt{2}$. Such a pattern is consistent with the presence of a mesophase adopting a discrete three-dimensional (3D) cubic structure.[32] Full elucidation of the structure of the cold phase incorporating RCs will require complementary small-angle neutron scattering studies.[8,33] The ability of the RCs to induce such a nonthermotropic phase transition is consistent with their known tendency to be stabilized, within a prolate or spherical detergent micelle.[34] On the basis of the NMR and small-angle diffraction studies, we conclude that above the phase transition the RC-doped compositions retain an expanded lamellar structure (Figure 5), while for the cold phase an ordered cubic mesophase is observed. Thus, it is clear that the RCs, while not influencing significantly the gel phase structure, do cause the more dynamic, cold phase to undergo a phase transition to a higher order structure.

Native Membrane Protein Function. The photophysical activity of the complex fluid-encapsulated RCs was examined by transient absorbance spectroscopy. The nature of the complex fluids dictated the experimental approach. For these studies, site-specific mutagenesis was used to create a mutant RC (M252Trp → Val) in which a valine replaces the native tryptophan at position 252 in the M subunit, thus eliminating the binding of quinone at the Q_A site. This modification serves to stop electron transfer after reaching the $P^+H_A^-$ charge-separated state (Figure 1, panel a).[35−38] This results in the formation of a state that lasts for only ~10 ns (1/e lifetime), thereby allowing the RCs within the illuminated volume to return to the ground state and

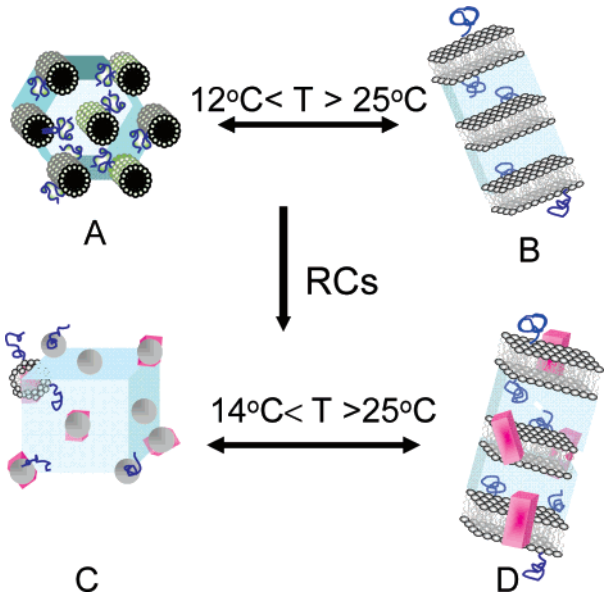

Figure 5. Schematic representation of the topology of polymer-grafted lipid-based complex fluid (A) in the cold, normal hexagonal phase, H_1, (B) above the phase transition, expanded lamellar structure, $L_{\alpha g}$, (C) doped with RCs below the phase transition, proposed cubic micellar phase, and (D) doped with RCs above the phase transition, expanded lamellar structure.

be available for subsequent excitation when the next laser pump pulse arrives 0.5 ms later. Such an approach is required to ensure that in subsequent flashes the RCs have returned to the ground state and are ready for the next electron-transfer cycle. An experimental strategy capable of completely refreshing the illuminated volume (of the sample) between laser flashes (e.g., by flowing or stirring the sample) was not possible since the proteo-complex fluids are viscous (especially above the phase transition) and highly ordered. In addition, slow diffusion in the lamellar phase prevented the use of a chemical regenerative system that has worked well for RCs studied in solution with high-repetition-rate laser systems.[39]

RC-specific activity was probed by monitoring the initial electron-transfer events ($P^* \rightarrow P^+H_A^-$) by transient absorption spectroscopy. Measuring the kinetics of the transient bleaching at 545 nm reveals the rate of loss of the ground-state absorption (Q_y transition) of H_A (Figure 6A, i). Kinetic traces at wavelengths other than 545 nm (e.g., at $\lambda \approx 650$ nm (Figure 6A, ii), corresponding to the formation of the H_A anion) were also studied (data not shown) and found to agree favorably.

The ultrafast transient data recorded on mutant RCs suspended in a detergent-micelle solution were compared with those of mutant RCs incorporated into either the low (10 °C) or the high (25 °C) viscosity states of the complex fluid and are presented in Figures 6A−C, respectively. The first transient spectrum, corresponding to P*, was taken immediately following the 838 nm pump pulse (at 1 ps, black); subsequent transients were recorded after $P^+H_A^-$ had formed (at 20 ps, red). The spectra recorded on the three RC samples reveal consistent features associated with the excited electron donor at early times and both the oxidized donor and the reduced acceptor during the later stages of the measurements. Small differences are noted in the amplitude of the "baseline" signals in the P* spectra on which the transient features originate. These deviations are believed to be unrelated to any RC photophysical process. These early signals may be indicative of varied solvent relaxation/reorganization processes in the three systems studied. Extensive further experimentation will be required to characterize fully

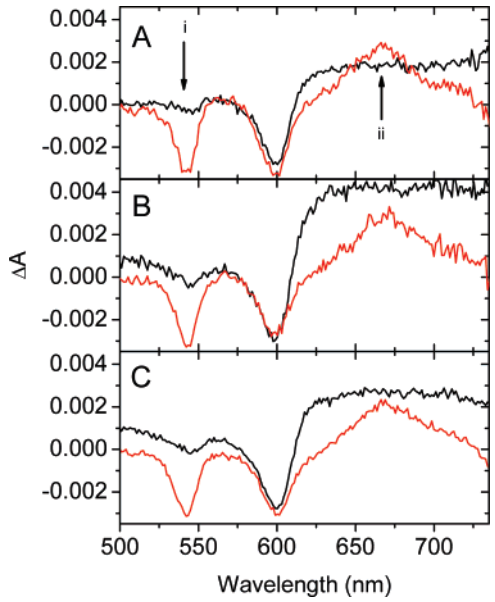

Figure 6. Transient spectra of mutant RCs suspended in a buffered, aqueous, detergent-micelle solution (A), in complex fluid at 10 °C (B), or in complex fluid at 25 °C (C). Data were recorded either immediately following the pump pulse (at 1 ps, black) or after the formation of $P^+H_A^-$ (at 20 ps, red). Arrows indicate wavelengths at which kinetic data were fit.

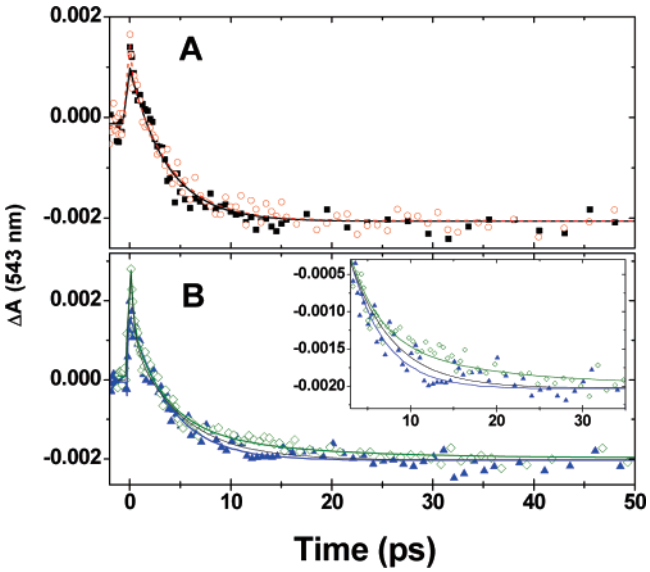

Figure 7. Comparison of kinetics of primary electron transfer (recorded at ~545 nm). (A) RCs suspended in a buffered, aqueous, detergent-micelle solution (black closed squares) versus those in complex fluid at 10 °C (red open circles). (B) Relatively dilute (11 μM, blue closed triangles) or more concentrated (18 μM, green open diamonds) RCs in the complex fluid after incubation at 25 °C for 3 h. Inset: Enlarged region of the data and fits emphasizing the need for extra kinetic components to model data from concentrated samples (one decay component, black; two decay components, green).

this effect. The close correspondence of the kinetically relevant, transient spectral features in all systems studied indicates that the natural function of the RC is intact.

Transient absorption data collected, at all RC concentrations, on proteo-complex fluids at 10 °C reveal kinetics with a monoexponential lifetime of 3.8 ps (Figure 7A, red), a value in excellent agreement with that measured for RCs in detergent micelles (Figure 7A, black). In addition, electron-transfer kinetics have been measured for a range of RC concentrations in the lamellar gel phase (at 25 °C, after equilibration for 15 min.). At the lowest concentration studied (10 μM), the lifetimes compare favorably with those observed for RCs in a buffered, aqueous solution of detergent micelles. In contrast, at the highest concentration studied (18 μM), a prolonged excited-state lifetime of the primary donor (P*), 5.4 ps, was observed. Increasing the equilibration time of the proteo-complex fluids in the lamellar gel phase extended the effective excited-state lifetime. These data sets were better modeled by including at least two distinct kinetic components, a short-lived component with a lifetime similar to the cold phase and solution RCs and a long-lived component with a lifetime exceeding 10 ps. The amplitude of the long component can represent up to 30% of the total decay (Figure 7B, Table 1). At lower RC concentrations, sample storage time in the gel phase did not affect the electron-transfer kinetics, displaying monoexponential ~3−4 ps lifetimes. Identical results were obtained for the samples independent of temperature or storage time (Table 1). It should be noted that although the data are fit well by a biexponential function a stretched exponential characteristic of an inhomogeneous distribution may be more appropriate (see below).

TABLE 1: Time Contants for the Primary Electron Transfer Observed in Mutant Reaction Centers (M252Trp → Val) Dispersed in Either a Buffered Aqueous Solution of Detergent Micelles or a Complex Fluid in the Liquid or Gel State

material	[RC] (μM)	T (°C)	t_{incb} (h)	τ (ps)[a] (A (%))
detergent micelles	18.2	10	0.25	3.6 (100)
		22	0.25	3.7 (100)
complex fluid	10.8	22	3	4.0 (100)
		22	29	4.1 (100)
complex fluid	13.6	10	0.25	3.2 (100)
		22	3	3.8 (100)
		22	29	4.0 (100)
complex fluid	18.2	10	0.25	3.9 (100)
		25	0.25	5.4 (100)
		25	3	2.7 (68)
				10.9 (32)

[a] The error calculated from replicated sample preparation and data acquisition was <10% of the fitted lifetimes that are reported (~3−4 ps). The error was slightly higher for more dilute samples with reduced signal-to-noise in the measurements.

The observed slowing of the rates of electron transfer at higher protein concentrations may originate either from effects inherent to the guest molecules (i.e., the RCs) or from guest/host interactions. Prior experimental and theoretical studies have suggested that the kinetics of primary electron transfer may deviate from simple exponential behavior.[40] Data collected on mutant RC complexes with substitutions near P, B_A, and/or B_B are particularly susceptible to such deviations. In addition, prior work has shown species dependence of this non-monoexponential behavior. For example, kinetics of primary electron transfer recorded on RCs derived from *R. sphaeroides* are predominantly observed to be monoexponential, while those from *R. capsulatus* (including WT) are commonly observed to be more complicated (as reviewed in ref 39 and references therein). These observations may be attributed either to the geometry and potential branched pathways (or mixtures of superexchange versus hopping of the electron from P to H_A^- through B_A)[24] or to distinct structural variants of individual RCs within the sample, each of which has a slightly different cofactor arrangement and thus a modified rate of primary electron transfer. Irrespective of the origin of the nonexponentiality, such possibilities can be discounted here because RCs in solution and in the cold phase exhibit the expected monoexponential kinetics. Furthermore, the increased lifetime is observed only with prolonged storage of the RCs in the lamellar gel phase

and is lost by cycling below the phase transition and rewarming to the gel phase. Thus, the matrix clearly has a role in affecting the observed kinetics.

The nature of the altered kinetics may arise from host−guest interactions with the complex fluid, perhaps by changing the conformational state of the RC and resulting in a statistical distribution of structural variants or by promoting the aggregation of the encapsulated protein. Prior work has shown that the local environment of the RCs can influence its electron-transfer kinetics. Specifically, extended lifetimes have been observed for monodisperse RCs in a variety of detergent micelles.[41] Although RCs are relatively robust, their kinetics for electron-transfer events can vary substantially with the detergent selected, with more complex behavior being observed in solutions that maintain the macromolecular assembly in a state closely resembling its native lipid-membrane environment.[41,42] In addition, there is evidence to suggest that artificial lipid (membrane) environments also regulate the RC function[43,44] through a variety of means, including alterations in protein flexibility and lipid binding to the surface of the proteins, which modifies physical parameters associated with charge separation and charge recombination. For example, studies have shown that the electron transfer between Q_A and Q_B and charge recombination of $P^+Q_A^-$ and $P^+Q_B^-$ states are all significantly faster for RCs in a synthetic lipid bilayer environment vs RCs in a buffered, aqueous solution of detergent micelles.[44] Thus, for our work, the possibility cannot be ruled out that the complex fluid alters the observed RC kinetics, giving rise to the observed time-dependent behavior. Alternatively, slowed rates of primary electron transfer have been measured in RCs in antennae-depleted chromatophores from *Rhodobacter* deletion strains.[22] In this environment, however, the possibility of protein aggregation influencing the observed kinetics could not be discounted. Interestingly, it is noted that the kinetics observed from RCs in the lamellar state of the artificial scaffold more closely mimic those observed for RCs in native membranes (chromatophores).

The potential for protein aggregation has been suggested in DMPC liposomes where the lipid chain order−disorder phase transition (L_β to L_α) is believed to promote a state whereby protein−protein interactions increase due to protein segregation. Lateral (in-plane) organization of photosynthetic assemblies has been imaged by atomic force microscopy and electron microscopy and has been shown to occur under select (e.g., native membrane, PufX, full complement of antennae) experimental conditions.[45−48] Confinement in the "sheetlike" structure afforded by the lamellar phase of the complex fluid may offer an ideal environment for the assembly of similar aggregates of RCs. It is conceivable that such an aggregated RC state could allow for excited-state energy transfer to compete effectively with primary charge separation. The excited-state energy may "hop" between neighboring RCs in the (in-plane) aggregate prior to being used to form the charge-separated state, thus leading to the observed extended effective lifetime. Most interestingly, the kinetics of the long-lived component observed in the RC-doped complex fluids resemble those observed in the isolated D1-D2 RC protein from Photosystem II (PS II) from higher plants.[49] In the PSII RC there are six chlorophyll *a* molecules and two pheophytin *a* molecules whose electronic spectra all overlap strongly. The two chlorophyll *a* molecules that make up the P680 primary electron donor interact electronically to a significant degree with the remaining six pigments in the reaction center complex, making it difficult to cleanly separate in a kinetic sense energy transfer between the pigments within the RC and electron transfer. In the D1-D2 protein, the measured time constant for primary charge separation is ca. 8 ps, which is significantly slower than the intrinsic time constant for charge separation due to rapid bidirectional excitation energy transfer among the pigments in the PSII RC.

Conclusions

The introduction of photosynthetic RCs into PEGylated, lipid-based complex fluids has been found to have little influence on the lamellar gel phase architecture of the fluid but does significantly alter the cold phase, converting it from a 2D hexagonal to a discrete 3D cubic structure. The RCs have been shown to remain structurally and functionally intact upon reconstitution into complex fluids. Specifically, in the cold phase of the complex fluid, primary electron-transfer kinetics are found to be identical to those of detergent-micelle-stabilized RCs under all conditions studied. At a threshold concentration, RCs in the warm, lamellar gel phase of the complex fluids show an extended lifetime. In addition, prolonged equilibration (hours) of the RCs in the lamellar gel phase results in multi-exponential kinetics of primary electron transfer, with a subpopulation of RCs displaying extended excited-state lifetimes that most likely arise from host−guest interactions, particularly those that promote the formation of reversible protein aggregates. The slow evolution of the signals observed from the concentrated, RC-doped, lamellar gels toward biexponential electron-transfer kinetics may arise from the lateral diffusion of monodisperse RCs intercalated into the "sheetlike" architecture of the lamellae, leading to the formation of RC-rich and RC-depleted regions. Although considerable work remains to fully understand the factors and conditions that control protein−protein and protein−host interactions in the complex fluids, a small subset of experimental conditions has been defined that leads to extended lifetimes, thereby identifying concentration ranges and time-dependent behaviors that influence the properties of the protein-doped materials. In addition, this work suggests the possibility of designing materials that further promote lateral "in-plane" segregation as a means to actively control the collective properties of reconstituted proteins. These areas as well as further characterization of the orientation and in-plane organization of the RCs in the lamellar gel phases will be the focus of future studies.

Acknowledgment. This work was performed under the auspices of the Office of Basic Energy Sciences, Divisions of Materials Sciences, United States Department of Energy, under Contract No. W-31-109-ENG-38. We gratefully acknowledge the help of Sönke Seifert in collecting the SAXS data.

References and Notes

(1) Hampp, N. *Chem. Rev.* **2000**, *100*, 1755−1776.
(2) Stuart, J. A.; Marcy, D. L.; Wise, K. J.; Birge, R. R. *Synth. Met.* **2002**, *127*, 3−15.
(3) Das, R.; Kiley, P. J.; Segal, M.; Norville, J.; Yu, A. A.; Wang, L. Y.; Trammell, S. A.; Reddick, L. E.; Kumar, R.; Stellacci, F.; Lebedev, N.; Schnur, J.; Bruce, B. D.; Zhang, S. G.; Baldo, M. *Nano Lett.* **2004**, *4*, 1079−1083.
(4) Subramaniam, V.; Alves, I. D.; Salgado, G. F. J.; Lau, P. W.; Wysocki, R. J.; Salamon, Z.; Tollin, G.; Hruby, V. J.; Brown, M. F.; Saavedra, S. S. *J. Am. Chem. Soc.* **2005**, *127*, 5320−5321.
(5) Holden, M. A.; Bayley, H. *J. Am. Chem. Soc.* **2005**, *127*, 6502−6503.
(6) O'Neill, H.; Greenbaum, E. *Chem. Mater.* **2005**, *17*, 2654−2661.
(7) Gelbart, W. B.; Ben-Shaul, A. *J. Phys. Chem.* **1996**, *100*, 13169−13189.
(8) Firestone, M. A.; Thiyagarajan, P.; Tiede, D. M. *Langmuir* **1998**, *14*, 4688−4698.
(9) Firestone, M. A.; Seifert, S. *J. Phys. Chem. B* **2000**, *104*, 2433−2438.

(10) Firestone, M. A.; Wolf, A. C.; Seifert, S. *Biomacromolecules* **2003**, *4*, 1539−1549.
(11) Firestone, M. A.; Tiede, D. M.; Seifert, S.; Thiyagarajan, P. *Div. Fuel Chem. Symp. Prepr.* **2000**, *45*, 375−379.
(12) Pokkuluri, P. R.; Laible, P. D.; Deng, Y. L.; Wong, T. N.; Hanson, D. K.; Schiffer, M. *Biochemistry* **2002**, *41*, 5998−6007.
(13) Taguchi, A. K. W.; Stocker, J. W.; Alden, R. G.; Causgrove, T. P.; Peloquin, J. M.; Boxer, S. G.; Woodbury, N. W. *Biochemistry* **1992**, *31*, 10345−10355.
(14) Kirmaier, C.; Laible, P. D.; Czarnecki, K.; Hata, A. N.; Hanson, D. K.; Bocian, D. F.; Holten, D. *J. Phys. Chem. B* **2002**, *106*, 1799−1808.
(15) Sinks, L. E.; Wasielewski, M. R. *J. Phys. Chem. A* **2003**, *107*, 611−620.
(16) Deisenhofer, J.; Epp, O.; Miki, K.; Huber, R.; Michel, H. *Nature* **1985**, *318*, 618−624.
(17) Allen, J. P.; Feher, G.; Yeates, T. O.; Komiya, H.; Rees, D. C. *Proc. Natl. Acad. Sci. U.S.A.* **1987**, *84*, 5730−5734.
(18) Chang, C.-H.; El-Kabbani, O.; Tiede, D. M.; Norris, J. R.; Schiffer, M. *Biochemistry* **1991**, *30*, 5352−5360.
(19) Ermler, U.; Fritsch, G.; Buchanan, S. K.; Michel, H. *Structure* **1994**, *2*, 925−936.
(20) Arnoux, B.; Gaucher, J. F.; Ducruix, A.; Reiss, F. *Acta Crystallogr., Sect. D* **1995**, *51*, 368−379.
(21) Stowell, M. H. B.; McPhillips, T. M.; Rees, D. C.; Soltis, S. M.; Abresch, E.; Feher, G. *Science* **1997**, *276*, 812−816.
(22) McAuley-Hecht, K. E.; Fyfe, P. K.; Ridge, J. P.; Prince, S. M.; Hunter, C. N.; Isaacs, N. W.; Cogdell, R. J.; Jones, M. R. *Biochemistry* **1998**, *37*, 4740−4750.
(23) Kirmaier, C.; Holten, D. *Photosynth. Res.* **1987**, *13*, 225−260.
(24) Woodbury, N. W.; Allen, J. P. In *Anoxygenic Photosynthetic Bacteria*; Bauer, C. E., Ed.; Kluwer: The Netherlands, 1995; pp 527−557.
(25) DiMagno, T. J.; Laible, P. D.; Reddy, N. R.; Small, G. J.; Norris, J. R.; Schiffer, M.; Hanson, D. K. *Spectrochim. Acta, Part A* **1998**, *54*, 1247−1267.
(26) Firestone, M. A.; Seifert, S. *Biomacromolecules* **2005**, *6*, 2678−2687.
(27) Grasso, D.; Milardi, D.; La Rosa, C.; Rizzarelli, E. *New J. Chem.* **2001**, *25*, 1543−1548.
(28) Thurmand, R. L.; Lindblom, G.; Brown, M. F. *Biochemistry* **1993**, *32*, 5394−5410.
(29) Lee, Y. S.; Yang, J. Z.; Sisson, T. M.; Frankel, D. A.; Gleeson, J. T.; Aksay, E.; Keller, S. L.; Gunner, S. M.; O'Brien, D. F. *J. Am. Chem. Soc.* **1995**, *117*, 5573−5578.
(30) Firestone, M. A.; Williams, D. E.; Seifert, S. *Nano Lett.* **2001**, *1*, 199−200.
(31) Efremva, N. V.; Sheth, S. R.; Leckband, D. E. *Langmuir* **2001**, *17*, 7628−7636.
(32) Johnsson, M.; Barauskas, J.; Tiberg, F. *J. Am. Chem. Soc.* **2005**, *127*, 1076−1077.
(33) Firestone, M. A.; Tiede, D. M.; Thiyagarajan, P. In *Materials Research Using Cold Neutrons at Pulsed Neutron Sources*; Thiyagarajan, P., Trouw, F., Marzec, B., Loong, C.-K., Eds.; World Scientific: Singapore, 1999; pp 160−169.
(34) Roth, M.; Arnoux, B.; Ducruix, A.; Reiss-Husson, F. *Biochemistry* **1991**, *30*, 9403−9413.
(35) Plato, M.; Michel-Beyerle, M. E.; Bixon, M.; Jortner, J. *FEBS Lett.* **1989**, *249*, 70−74.
(36) Coleman, W. J.; Bylina, E. J.; Aumeier, W.; Siegl, J.; Eberl, U.; Heckmann, R.; Ogrodnik, A.; Michel-Beyerle, M. E.; Youvan, D. C. In *Structure and Function of Bacterial Photosynthetic Reaction Centers*; Michel-Beyerle, M. E., Ed.; Springer-Verlag: New York, 1990; pp 273−281.
(37) Stilz, H. Y.; Finkele, U.; Holzapfel, W.; Lauterwasser, C.; Zinth, W.; Oesterhelt, D. In *Structure and Function of Bacterial Photosynthetic Reaction Centers*; Michel-Beyerle, M. E., Ed.; Springer-Verlag: New York, 1990; pp 265−271.
(38) Stilz, H. U.; Finkele, U.; Holzapfel, W.; Lauterwasser, C.; Zinth, W.; Oesterhelt, D. *Eur. J. Biochem.* **1994**, *223*, 233−242.
(39) Laible, P. D.; Greenfield, S. R.; Wasielewski, M. R.; Hanson, D. K.; Pearlstein, R. M. *Biochemistry* **1997**, *36*, 8677−8685.
(40) Bixon, M.; Jortner, J.; Michel-Beyerle, M. E. *Chem. Phys.* **1995**, *197*, 389−404.
(41) Wang, S.; Lin, S.; Woodbury, N. W.; Allen, J. P. *Photosynth. Res.* **1994**, *42*, 203−215.
(42) Kirmaier, C.; Laible, P. D.; Hindin, E.; Hanson, D. K.; Holten, D. *Chem. Phys.* **2003**, *294*, 305−318.
(43) Hanson, D. K.; Tiede, D. M.; Nance, S. L.; Chang, C.-H.; Schiffer, M. *Proc. Natl. Acad. Sci. U.S.A.* **1993**, *90*, 8929−8933.
(44) Tally, A.; Baciou, L.; Sebban, P. *FEBS Lett.* **2002**, *532*, 91−96.
(45) Bahatyrova, S.; Frese, R. N.; Siebert, C. A.; Olsen, J. D.; Van Der Werf, K. O.; Van Grondelle, R.; Niederman, R. A.; Bullough, P. A.; Otto, C.; Hunter, C. N. *Nature* **2004**, *430*, 1058−1062.
(46) Fotiadis, D.; Engel, A. *Methods Mol. Biol.* **2004**, *242*, 291−303.
(47) Scheuring, S.; Francia, F.; Busselez, J.; Melandri, B. A.; Rigaud, J. L.; Levy, D. *J. Biol. Chem.* **2004**, *279*, 3620−3626.
(48) Scheuring, S.; Busselez, J.; Levy, D. *J. Biol. Chem.* **2005**, *280*, 1426−1431.
(49) Greenfield, S. R.; Govindjee; Seibert, M.; Wasielewski, M. R. *J. Phys. Chem. B* **1997**, *101*, 2251−2255.